Gaseous Discharge Plasmas Produced by High-Energy Electron-Irradiated Insulators for Spacecraft

Arthur Robb Frederickson, *Senior Member, IEEE*, C. E. Benson, and E. M. Cooke

***Abstract*—High-energy electron irradiation of insulators in vacuum causes both internal regions and surfaces of insulators to achieve high (negative) static voltage relative to nearby "ground." Occasional spontaneous discharges inject pulses of partially ionized gas composed of the insulating material and surface gas-adatoms into the adjacent vacuum. The gas is capable of partially discharging the high surface potentials by carrying current across the vacuum to "ground." The current-time waveforms were measured as a function of the spatial arrangement of the sample, test chamber electrodes, and static electric fields in order to investigate effects inside spacecraft boxes and cavities. It was found that plane-parallel electric fields are less able to sustain large discharge currents than are divergent electric fields. Also, physical confinement of the pulse of gas within the region of the electric field greatly increases the conductance of the gaseous discharge. Thus, the spatial arrangement of the sample, test chamber electrodes, and static electric field has a strong impact on the level of ESD-pulse threat to sensitive electronics posed by spontaneous discharges of irradiated insulators in spacecraft.**

I. Introduction

In the 1970s, it was determined that spacecraft were experiencing transient events or anomalies when the spacecraft experienced elevated fluxes of high-energy electrons in the magnetosphere plasma [1]. For at least ten years, a strong international effort pursued the problem under the rubrics of Spacecraft Charging or Spacecraft Anomalies. Since spacecraft used extensive thermal control surfaces made of polymers (usually coated with a film of metal on the inner surface) such as Kapton or Teflon, these materials were suspected of producing discharge pulses when passing through regions of high energy electron fluxes, typically where geosynchronous communications spacecraft orbit.

The SCATHA spacecraft was flown to investigate these effects, and it recorded high surface voltages, several kilovolts, on thermal blanket material relative to the frame of the spacecraft. Charged particle spectrometers detected that the cold positive ions were accelerated into the spacecraft which indicated that the frame of the spacecraft was sometimes negatively charged (up to 10 kV) relative to ambient [2]–[7]. A transient pulse monitor detected electrical discharges by the spacecraft. The discharges could occur from spacecraft to ambient, or between electrically isolated portions of the spacecraft at different voltages [8]–[11].

The CRRES spacecraft was instrumented to monitor pulses produced by insulators inside the spacecraft [12], [13]. The insulators were charged by space electrons with energies exceeding 150 keV which could pass through a 0.2-mm-thick grounded aluminum foil and stop in the insulating material. Lower energy electrons were stopped or reflected by the foil. The pulse history of the insulators was recorded and correlated with the history of high-energy electron flux monitored by particle spectrometers on the spacecraft [14]. Different materials behaved differently with respect to electron flux and aging.

The SCATHA and the CRRES spacecraft proved that standard insulating materials produce pulses when experiencing high-energy electrons in space. But oscilloscopes were not flown and the pulse shapes are mostly unknown [14]. Ground tests of the same kinds of samples were able to measure the pulse-shapes and amplitudes while irradiating with electrons from several kilovolts to several megavolts [13], [15]–[18]. In reviewing the reported pulses in many of the ground tests, it was determined that the pulse shapes and amplitudes may depend on the geometry of the test chamber [19]. But only a controlled set of experiments would be able to demonstrate how the geometry affected the pulse shapes. This paper investigates the pulse shapes as the spatial arrangement of the sample, test chamber electrodes, and static electric field adjacent to the charged insulator is varied.

That partially ionized gas is involved in the discharge process had been previously noted [20]–[22]. The amount of gas produced by some discharges from Mylar has been measured to be of order 0.1 mm^3 at STP [23]. The gas is able to form a strong current flow of hundreds of amperes with only a 100-V source in the vacuum near the sample [23]. In the experiments of [23], the vacuum chamber was small allowing the pulse of gas to be observed in the vacuum gauge and in the transient monitor on the electron gun power supply. Of the numerous (a thousand?) pulses, every one produced a gas pulse as monitored on a strip chart recorder attached to the vacuum gauge, and nearly every one caused the 20-kV gun power supply to trip off. In the new experiments reported now, and in many others we have observed in *large* vacuum chambers, the vacuum gauges do not record the pulses and the guns do not usually trip off because: 1) the large chamber absorbs the pulse of gas without measurably deflecting

Manuscript received February 16, 2000; revised September 21, 2000. This work was supported by the National Aeronautics and Space Administration and the Space Environment Effects Program at MARSHALL Space Flight Center.

A. R. Frederickson and C. E. Benson are with the Jet Propulsion Lab, California Institute of Technology, Pasadena, CA 91109 USA.

E. M. Cooke is with the Electrical Engineering, University of Wisconsin, Madison, WI 53706 USA.

Publisher Item Identifier S 0093-3813(00)11343-8.

0093–3813/00$10.00 © 2000 IEEE

the vacuum gauge and 2) the pulsed plasma density at the gun is not sufficient to develop a secondary breakdown at the gun electrodes.

Pulse amplitude and shape are very important because they determine the level of threat imposed upon the spacecraft electronics. The static energy available in the charged-up samples is substantial, sometimes exceeding a joule (up to 10 kV on microfarads). Typical circuit board pulses coupled into 50-Ω lines often deposit millijoules into the 50-Ω load. Some modern electronic devices fail under microjoule pulses above 20 V. The effectiveness of filtering and decoupling depend upon the shape and amplitude of the pulses.

II. Approach

The effects of changed material geometry, of changed electric field profiles, and of constrained gas trajectories are investigated by changing the arrangement of grids and material walls adjacent to the charged insulator surface. The irradiating electrons pass through the grids to charge the insulator samples. But the electric fields are terminated as desired by metal grids, chamber walls, and thin metal foils. Gas particle trajectories are partially constrained by grids of varying optical density, or by electric fields.

Insulating materials on spacecraft occur in several configurations. Materials on the outer surface will discharge to space plasma or to adjacent materials on the surface. Space electrons at energies above 50 kV will pass through thermal control blankets and irradiate insulator materials such as wire bundles, struts, connectors, battery boxes, etc. These materials will discharge to the grounded metal surfaces nearby such as the back metal on thermal blankets, electronic boxes, spacecraft frame, ground wires, etc. Electrons at energies above roughly 500 keV will penetrate into electronic boxes and charge electronic packaging, circuit boards, wire insulation, connectors, etc. Each of these items will discharge to other materials nearby. For the outermost circuit board the discharge will propagate to the box walls. Interior circuit boards will discharge into circuit wiring, or into other insulators nearby. In vacuum the electric fields will have many conformations from highly divergent to "laminar." The voltage differences will usually exceed a kilovolt, and in some cases achieve tens of kilovolts. Actual geometrical arrangements are exceedingly varied. This work investigates phenomena that relate to the shape of the vacuum space adjacent to the irradiated material.

It is important to maintain the samples constant during the many changes in spatial arrangement of the sample, test chamber electrodes, and static electric field. Because of their technological importance and extensive application in spacecraft, FR4 circuit board is the sample of choice. FR4 board is an epoxy fiberglass laminate of the fire retardant (FR) type. It is known to produce pulses in space application [14].

A. Experimental Apparatus

The basic irradiation chamber is described in Fig. 1. With the no samples in the chamber, but all other components intact, a two-day irradiation produced no pulses. Additionally, the

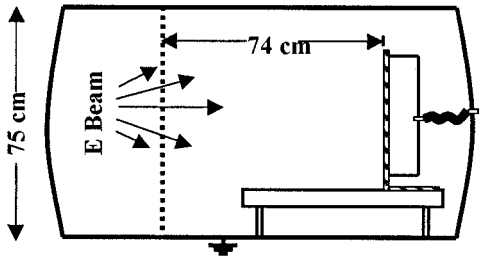

Fig. 1. *Vacuum chamber and electron flood gun*. The electron beam passes through the grounded accelerator anode screen and drifts before striking the samples. The wiring from the samples is shielded from the high-energy electrons so that the wiring does not itself contribute pulses. Vacuum levels ranged from 7×10^{-7} to 5×10^{-6} T.

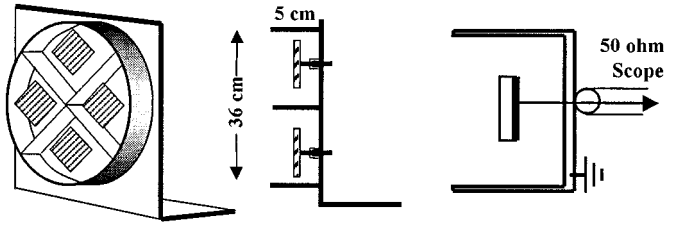

Fig. 2. *Mounting arrangement for four samples*. The signal wires soldered to the copper electrodes serve to mount the samples. The insulators which isolate the signal wire from ground are guarded from impact by scattered high-energy electrons. Perspective view of four samples is at the left. The cross section view in the center depicts how samples are electrically isolated from one another. The view on the right indicates the basic spatial arrangement of the sample, test chamber electrodes, and static electric field upon which all discussions are based. The scope is a Tektronix model TDS-544 A four channel transient digitizer. 50 Ω attenuators were used to prevent the signals from exceeding 500 V at the input to the scope. Positive signal corresponds to positive voltage on the center conductor of the coaxial line.

sample mounts and the wiring is arranged so that all of their surfaces exposed to the electron beam are metallic and grounded. Only the samples can be charged by the high-energy electrons. Four samples can be irradiated simultaneously. The intensity of the beam is reasonably uniform such that at the point of lowest intensity the flux is at least half the flux at the point of highest intensity.

The sample mounting arrangement is shown in Fig. 2. The samples are surrounded on five sides by grounded aluminum plates which are everywhere spaced at least 2.5 cm from the samples. The "front" faces of the samples are bombarded by the electron beam and the "back" faces are covered with the standard copper metal on circuit boards.

In the following discussions, the drawings are simplified to depict one sample at a time. However, all four samples are similarly arranged in each irradiation. In every case, the conductive barriers between samples prevent discharges on one sample from significantly coupling onto the adjacent samples. Only small radio frequency coupling was observed in these experiments. There have been cases noted in the literature where the gas or plasma from one sample discharged nearby samples [19], but this was not seen in the tests being reported here.

The FR4 material is irradiated in the normal direction by the high-energy electrons that stop inside the insulating material. The circuit board samples are 0.165 cm × 7.6 cm × 7.6 cm in size with standard copper sheet on the back side, and 0.06 cm × 6.7 cm × 6.7 cm with aluminum tape on the back side.

In all irradiations the incident 30-keV electrons penetrate approximately 0.0003 cm, only a small fraction of the thickness of the material, before coming to rest. Most of the (positive) image charge moves from ground through the 50 Ω scope to reside in the copper electrode on the back of the sample during irradiation, but a few percent of the image charge resides in the (conductive) mounting structure and the vacuum chamber walls [19]. The signal monitored by the scope consists only of image charges flowing in the scope wires during the pulses. Although the electric field in the insulation at the surface of the copper is large in these experiments, discharges occurring in this region produce only small signals on the scope [19] because the resulting image currents are small.

B. Electric Fields

The electric field in the vacuum is an important parameter which is adjusted in the experiments. Here we make only rough "eyeball" estimates of their vector magnitudes. The fringing regions will not be estimated. It is critical to know that the surface voltage of the samples is determined by the bombarding energy of the high-energy electrons. For monoenergetic normal incidence electrons, the surface potential will nearly achieve a (negative) voltage given by

$$V_s = eV_p - eV_{sc}$$

where

- V_s (negative) surface voltage;
- eV_p energy of incident electrons in electron volts;
- eV_{sc} "second crossover" energy at which the incident electron produces exactly one backemitted electron to leave the surface.

For insulators, eV_{sc} is typically in the range from 2 keV to 5 keV, depending on the sample.

The effect of nonnormal incidence is to increase eV_{sc} by a factor slightly greater than the secant of the angle from normal, perhaps up to five or so for glancing incidence. It is possible to self consistently determine the charging of a surface, its effect upon the trajectories and incidence angle of the electrons, the increase of backemitted electrons, and the resultant lowering of the final surface voltage. Such experiments (unpublished) were performed where surface voltage was measured for several geometries of electrodes in the vacuum. The net result from the experiments can be succinctly stated as follows.

1) When a grid is placed parallel and close (relative to the linear dimension of the sample) to the sample, the incident electron trajectories impact normal to the surface and the surface potential comes to exactly the prediction of the equation. For our samples, the resulting surface potential will be assumed to be roughly 3 kV below the energy of the incident electrons because the second crossover point is assumed to be at roughly 3 kV.
2) Without the grid, incident electrons will deviate from normal incidence and produce a potential assumed in this case to be 5 kV below the incident electron energy. For samples not encased in the wells shown in Fig. 2, the incident electrons would be further deflected and the surface potential would be approximately 10 kV below the incident beam energy.

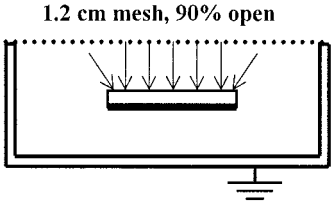

Fig. 3. *The plane-parallel high-field arrangement*. Arrows represent electric field.

These estimates are for beams between 25 and 35 keV. More accurate estimates are not helpful in these "first-cut" experiments.

Initially, the most negative voltage occurs at the depth of the average stopping point of the electrons in the insulator, a few microns for 30 keV electrons, and moves somewhat from that exact depth as conduction currents in the insulator redistribute charge. When a discharge occurs, the surface potential drops from perhaps −27 kV to typically −10 or −20 kV as positive ions from the discharge plasma arrive at the surface of the insulator and electrons escape to ground. The electric field in the first micron quickly increases, but not more than a factor of two. The electric field in the back of the sample decreases strongly. The process of charging and discharging maintains both a strong but varying field in the first few microns of the sample, as well as an oppositely directed strong and varying field in the back of the sample.

Fringing fields are always a concern when designing experiments and interpreting results in high voltage discharges. In this case, the fringing field is near the edge of the samples, between space charge in the insulator and image charge at the edge of the copper sheet. The field is also very large, but is partially mitigated by radiation-induced low-energy particle currents (exact magnitude unknown) near the edge of the insulator material. The effects of fringing fields are not yet determined. But in all of these experiments the fringing field remained relatively constant so that the variations in discharge pulses are mostly due to the variations in experimental conditions, and at most weakly related to fringing fields. Readers are encouraged to contribute their own thoughts to the issue of fringing fields. Real objects on spacecraft have fringing fields, so they must be studied.

III. Detailed Experiments

The experimental arrangements of materials and vacuum electric field profiles are varied as depicted in Fig. 3. The discharge pulses associated with each arrangement are described with an illustrative example along with a table describing each of the many pulses for that arrangement. The first group of tests is performed with the 0.165 cm × 7.6 cm × 7.6 cm FR4 samples.

A. First Arrangement

The first arrangement generates nearly parallel electric field in the vacuum with a 90% transmission grounded grid placed 2.5 cm from the surface. The incident electrons arrive at the surface in the normal direction, and the surface achieves up to

TABLE I
PULSES UNDER 90% TRANSMISSION GRID

Pulse number 10/04/99	Width at Half Peak (ns)	Peak current 50 ohms (A)	Charge (Coulombs)	Energy in 50 ohms (mJ)
1:48:48	160	8.8	1.67E-06	0.46
1:57:03	172	7.0	1.29E-06	0.31
2:08:08	236	5.7	1.35E-06	0.26
2:11:58	260	5.4	1.25E-06	0.21
2:15:58	138	11.4	1.41E-06	0.41
2:22:21	116	7.6	1.05E-06	0.20
2:27:06	224	6.3	1.55E-06	0.29
2:33:09	190	5.1	1.10E-06	0.17
2:36:24	278	4.0	1.28E-06	0.16
2:41:56	248	5.1	1.32E-06	0.21
2:48:27	196	5.7	1.52E-06	0.24
2:55:55	250	5.1	1.37E-06	0.21
3:00:10	236	5.1	1.10E-06	0.15
3:07:37	260	4.6	1.30E-06	0.18
3:12:26	316	3.8	1.25E-06	0.15
3:18:07	264	4.4	1.33E-06	0.17
3:38:34	300	4.4	1.42E-06	0.17
4:39:41	264	5.1	1.43E-06	0.21
Average	228	5.8	1.33E-06	0.23

−27 kV when bombarded by initially 30 keV electrons. Most of the vacuum field is plane-parallel as shown by the arrows in Fig. 3.

All of the pulses captured in one run are listed in Table I. The trigger level on the scope was set so that most pulses were fully recorded. Prior tests had taught us that by setting the scope to be more sensitive, very few small pulses are seen and most of the pulses are then off scale. Another full 8-h run found no negative pulses. Negative pulses occur when the discharge passes through the fringing field region onto the sample electrode thus causing positive image charges originally in the aluminum sample holder to flow through the scope onto the sample copper electrode. One must choose which polarity triggers the scope.

The beam current was approximately 0.5 nA/cm^2. Over the three orders of magnitude of beam current used on our tests, the discharge pulse shape and amplitude do not depend upon beam current. The frequency of pulsing, however, strongly depends upon beam current, although not necessarily linearly.

It is instructive to roughly estimate the time to charge the sample. Pulses are identified in Table I by their times of occurrence during the two hour test. The surface capacitance, C, to "ground" is 2.33 pF/cm^2. Assume that, on average during charging, half of the incident current is backemitted and half is absorbed near the front surface of the insulator. Using $dV/dt = I/C, I = 0.25$ nA/cm^2, one finds that $dV/dT = 107$ V/s, approximately. Thus, a discharge of 12 kV requires about 2 min to recharge. Therefore, the time to recharge the samples will play a role in the pulse history when pulses occur within about five minutes of each other. Inspection of the extensive data sets, much of which is not listed in this paper, indicates that this sometimes happens.

The scope has captured a number of pulses that occured within 10 ms of a first pulse, and data from CRRES [14] found

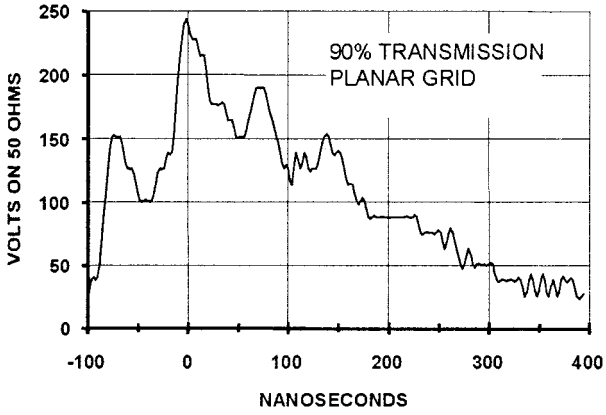

Fig. 4. A Typical pulse using the 90% transmission plane-parallel grid at 2.5 cm above the sample surface.

second pulses frequently occur before substantial recharging occurs. The surfaces were charged initially to 20 kV or more. During the pulses the voltage typically dropped roughly 10 kV. Thus, many kilovolts, typically ten, remain to generate a second pulse immediately after a first pulse, providing further evidence of a weak discharge process limited by the amount of gas and not by surface voltage.

It is also instructive to evaluate the amount of surface voltage eliminated by the discharges. The capacitance of the surfaces of these insulator samples to the copper substrate is 2.33 pF/cm^2, and for the entire sample is 135 pF. From the equation $CV = Q$, we find that the average pulse in Table I changed the surface voltage by 9.85 kV. The pulse with largest total current dropped the voltage by 12.37 kV.

A typical pulse is shown in Fig. 4. The pulses with the plane-parallel 90% transmission grid are often jagged. It appears that the discharge is not well-organized, as if the discharge process nearly quenches several times during the pulse. Despite the fact that the electric field is large, perhaps 10 kV/cm at the beginning of the pulse, the discharge process is "weak." A strong discharge would drop the surface well below a kilovolt. The fact that the surface voltage typically decays by 10 kV when the surface was initially above 20 kV is further evidence that the discharge process is "weak." Such a discharge is reminiscent of a diffuse gas discharge, or other weak process. Certainly this is not strong like a gas arc switch, nor a lightning arrestor, nor a voltage regulator tube!

What might be the cause for the quenching and weakness of the pulses in the presence of the 90% transmission grid? The effect of the grid might be to allow neutral gas molecules to pass through the grid and out of the high-field region before becoming ionized in the Townsend avalanche. The escaping molecules would not contribute to discharge current. This idea can be investigated by making the grid much more dense in order to block much of the out-diffusion of gas and keep it in the high-field region longer. The second arrangement tests this idea.

Electrons and ions having passed through the plane of the grid have fully contributed to the discharge current independent of whether they stop on the grid or continue to the far walls of the chamber, or forever drift between the chamber walls

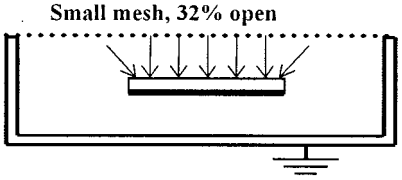

Fig. 5. Arrangement for plane parallel 32% transmission grid, similar to Fig. 3. Arrows indicate E-field.

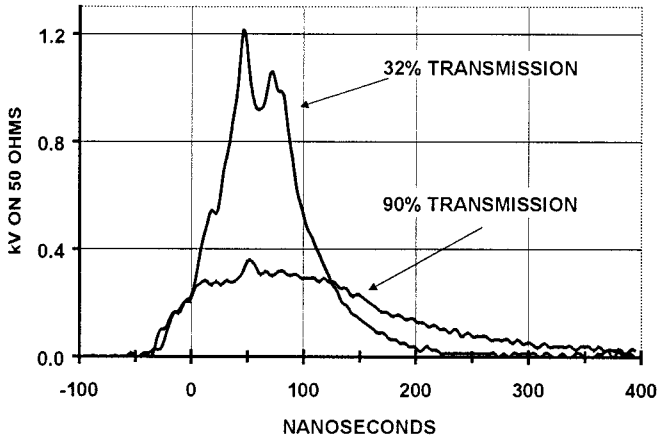

Fig. 6. Comparison of a pulse using the 90% transmission plane-parallel grid to a pulse using the 32% transmission plane-parallel grid.

and the grid. It is the image charges in the grid and chamber and other "grounded" objects that constitute the current flows in the ground circuit. For nearly every charged particle which passes from the surface of the insulator to the plane of the grid, there is an oppositely charged image charge flowing from the sample electrode through the 50 Ω scope and onto the system of grounded electrodes (which includes the vacuum chamber, grounded grids, earth ground, etc).

B. Second Arrangement

A similar experiment was performed on the same samples with a dense grid of 32% transmission also placed 2.5 cm above the sample surface, shown in Fig. 5. Because the grid blocks some incident electrons, the electron beam intensity is adjusted to produce the same intensity at the surface of the sample.

Fig. 6 succinctly describes how the results changed. Table II lists all of the pulses in one test using the dense grid. It is very clear that partial confinement of the neutral gas provided the following results on average:

1) more complete discharge of the surface voltage, here an average of 13.7 kV compared to 9.85 kV;
2) a stronger gas discharge current with much less evidence of quenching;
3) higher average peak current by a factor of 3.6, here an average of 20.7 A compared to 5.8 A.

Thus, the average pulse reduced the surface voltage by 13 700 volts and the largest pulse reduced it by 16 100 V.

Before continuing with gas discharge studies, it is important to consider the practical implications of these results. The circuit board is a model of a typical electronic board, or IC package, or antenna insulator substrate. The 50-Ω oscilloscope is a model of a sensitive circuit on the spacecraft. Although the many spacecraft circuits have many impedances to ground, it is instructive to directly use the 50-Ω data for the moment. The spatial arrangement of the sample, test chamber electrodes, and static electric field and the gas discharge dynamics strongly affect the following engineering parameters:

1) peak voltage delivered to the sensitive circuit. (290 V versus 1035 V);
2) peak current flowing in the circuit. (5.8 A versus 20.7 A);
3) power radiated into radio frequencies and its distribution in frequency (see Fig. 6 for indication of this effect);
4) power/energy delivered to the sensitive circuit (1.7E3 W peak versus 2.1E4 W peak; or integrated over the time-waveforms, 0.23 mJ versus 1.1 mJ).

Thus, such a change in the spatial arrangement of the sample, test chamber electrodes, and static electric field has a large effect upon the threat developed by discharge pulses. Such geometrical effects are not normally considered when evaluating the threat to spacecraft. The following tests were performed to more thoroughly evaluate the threat as geometry is changed. In addition such studies help one to evaluate the relation of testing geometry to the real geometry.

TABLE II
PULSES UNDER 32% TRANSMISSION GRID

Pulse number 9/21/99	Width at Half Peak (ns)	Peak current 50 ohms (A)	Charge (Coulombs)	Energy in 50 ohms (mJ)
1:00:38	64	28.4	2.17E-06	1.92
1:03:18	66	24.0	2.03E-06	1.48
1:06:00	80	24.0	1.97E-06	1.56
1:09:22	86	23.4	2.02E-06	1.57
1:14:27	82	22.1	2.02E-06	1.46
1:17:51	76	22.1	2.00E-06	1.37
1:26:05	92	22.1	1.97E-06	1.35
1:32:50	94	20.2	1.96E-06	1.16
1:36:10	104	17.7	1.80E-06	1.10
1:48:22	38	26.5	1.83E-06	1.20
1:57:49	108	15.2	1.83E-06	0.81
2:12:10	48	20.2	1.80E-06	0.93
2:27:20	58	20.2	1.76E-06	1.01
2:40:01	58	17.1	1.67E-06	0.79
2:49:58	98	16.4	1.69E-06	0.84
2:57:18	66	17.7	1.61E-06	0.85
3:08:35	76	17.1	1.63E-06	0.78
3:32:52	92	17.7	1.63E-06	0.67
Average	77	20.7	1.85E-06	1.10

C. Third Arrangement

The effect of smaller electric field in vacuum might be important. The grids in the prior two tests, being placed only 2.5 cm from the sample surfaces and parallel to the surfaces produce high vacuum electric fields, 27 kV/2.5 cm = 11 kV/cm.

The electric field was made smaller by removing the grid, and placing the sample as far from all grounds as possible. However, the back sample electrode, which is at ground potential when a pulse is not occurring, remains at the sample and one can visualize strong fringing fields to this electrode. The arrangement is depicted in Fig. 7, and only one sample is mounted.

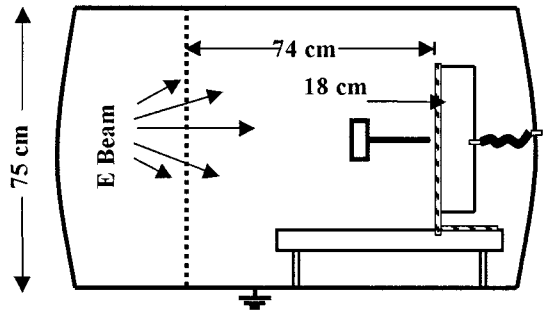

Fig. 7. Single sample is mounted 18 cm from the nearest vacuum chamber grounds to reduce the electric field in vacuum.

TABLE III
PULSES FROM SAMPLE SUSPENDED MIDCHAMBER WITHOUT GRIDS

Pulse number 7/16/99	Width at Half Peak (ns)	Peak current 50 ohms (A)	Charge (Coulombs)	Energy in 50 ohms (mJ)
9.31.57	40	18	1.4E-06	0.6
9.34.05	50	18	2.0E-06	0.8
9.39.54	48	23	1.9E-06	1.1
10.19.06	36	24	2.2E-06	1.0
10.25.05	40	28	2.0E-06	1.3
10.29.20	80	17	2.1E-06	0.9
10.40.58	82	23	2.1E-06	1.2
10.45.47	76	21	2.2E-06	0.9
10.48.26	96	18	2.2E-06	1.0
11.04.40	56	19	2.1E-06	0.9
11.10.24	46	32	2.2E-06	1.7
11.20.33	54	25	2.2E-06	1.4
11.25.41	34	32	2.1E-06	1.5
11.36.14	36	32	2.2E-06	1.5
11.40.17	48	25	2.2E-06	1.2
11.44.36	60	26	2.1E-06	1.3
11.56.29	42	30	2.1E-06	1.5
12.00.25	56	26	2.1E-06	1.4
12.09.57	44	30	2.1E-06	1.5
Average	54	25	2.1E-06	1.2

The sample is roughly 18 cm from both its mounting plate, and from the base plate grounds. Presumably the maximum charging voltage is 25 kV so that the field strength averages roughly 20/18 = 1.1 kV/cm, much lower than the previous 11 kV/cm. Of course, the field distribution is complex, being largest near the sample, but has not been analyzed.

If the strength of the discharge is proportional to electric field strength, and to confinement of neutral gas, one should see diminished pulse amplitudes relative to both prior experiments. The results are presented in Table III, and a typical pulse for the third arrangement is seen in Fig. 8. It is clear that the pulses in the third arrangement are as strong (or stronger) as those in the second arrangement. The surface voltage lost in a discharge is 15 500 V on average, and 16 300 V in the largest pulse.

Moving the sample far from a planar grid or other planar electrode may cause the divergence of the vacuum electric field to become important. A divergent electric field produces a force on a polarizable neutral gas molecule proportional to the divergence of the electric field. As neutral gas atoms leave the sample surface they initially experience negligible divergence

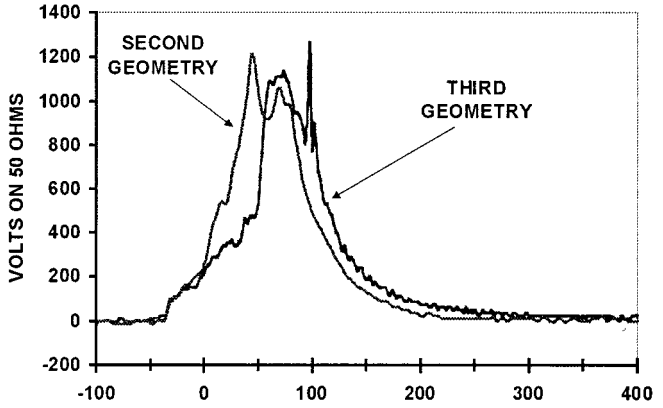

Fig. 8. Pulse under fully open arrangement of Fig. 7 compared to pulse under 32% transmission planar grid.

of the electric field. Since the planar sample surface is roughly 7-cm wide, the divergence of electric field will have maximum effect several cm to 10 cm from the surface. (Fringing fields have much stronger divergence but occupy small spatial volume and thus affect fewer gas molecules.) The diverging fields may prevent the polarizable gas molecules from escaping beyond a few cm from the surface of the charged sample. Perhaps the divergent static electric fields confine much of the gases that escape from FR4 circuit board during discharge events. Order of magnitude estimate on this effect is provided in the Appendix.

Additionally, one might hypothesize that the thermalized neutral molecules take time to transit to the walls of the vacuum chamber and thus are longer exposed to the current avalanche process in the arrangement without any grid. The results of tests in the fourth arrangement indicate that this may not be as important as the hypothesis of gas confinement by field gradient, but these tests do not rule out the argument.

During the discharge the magnetic field and space charge field probably play a very important role. This experimental study is programatically constrained to make only a first cut set of measurements to determine the magnitude of pulses from typical spacecraft electronics, and develop concepts for how strongly the discharges couple into circuits. Instead of performing a detailed scientific analysis of the gas and discharge plasma phenomena, we are constrained to using first order concepts to search for worst-case phenomena for engineering design purposes.

Unfortunately, the samples from this point forward are not the same as previous tests. The samples in Table IV and beyond are FR4 circuit boards of thickness 0.059 cm, dimensions of 6.7 $\times$ 6.7 cm. The rear electrode of these samples was composed of conductive aluminum cloth adhesive tape such that the cloth and adhesive were of significant thickness to alter the capacitance of the irradiated surface to the sample electrode. The measured surface capacitance is 178 pF for the samples, or 4.0 pF/cm^2.

D. Fourth Arrangement

Based on the previous three experiments, and the previous phenomenological explanations, a fourth arrangement is proposed as a worse situation. A conical grid is placed near the sample in order to maximize both the field strength and its divergence, and thereby hold the neutral molecules close to the

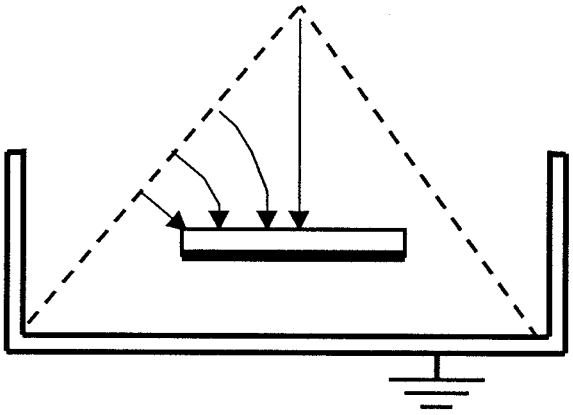

Fig. 9. Experiment with the 60% transmission conical grid. The peak of the cone is 5.5 cm above the sample surface. The arrows indicate a divergent E-field with maximum strength near the sample surface.

TABLE IV
PULSES UNDER CONICAL GRID

Pulse number 11/26/99	Width at Half Peak (ns)	Peak current 50 ohms (A)	Charge (Coulombs)	Energy in 50 ohms (mJ)
11.19.21	130	23	4.6E-06	2.6
11.24.30	88	12	1.8E-06	0.5
11.25.00	196	7	1.8E-06	0.3
11.39.27	96	12	1.6E-06	0.5
11.40.03	136	34	5.7E-06	4.4
11.42.35	110	11	1.8E-06	0.4
11.52.42	100	11	1.7E-06	0.5
11.56.43	106	30	5.0E-06	3.7
12.00.52	120	13	2.0E-06	0.6
12.10.01	60	16	1.9E-06	0.7
12.10.19	276	21	5.6E-06	3.4
12.22.34	110	13	2.2E-06	0.7
12.24.02	150	25	5.1E-06	3.2
12.26.36	172	10	1.7E-06	0.5
12.37.52	154	24	4.8E-06	2.6
12.45.28	172	11	2.3E-06	0.7
12.48.19	86	19	2.2E-06	1.1
12.50.31	110	21	4.0E-06	1.8
1.01.55	128	8	1.7E-06	0.3
1.03.26	182	7	1.3E-06	0.2
1.06.50	122	31	5.5E-06	3.9
1.14.49	154	7	1.3E-06	0.2
1.22.10	108	9	1.5E-06	0.4
1.23.47	106	30	5.0E-06	3.2
1.27.58	194	5	1.2E-06	0.1
1.39.33	104	12	1.6E-06	0.5
1.42.33	54	36	5.0E-06	3.4
1.43.25	154	7	1.2E-06	0.2
1.55.12	188	7	1.6E-06	0.3
2.00.26	54	36	5.2E-06	3.7
2.02.18	124	15	2.1E-06	0.7
Average	130	17	2.9E-06	1.5

sample and expose them to a more active Townsend avalanche. Fig. 9 displays the conical grid arrangement.

The results for the conical grid are provided in Table IV. The samples were 0.06 cm × 6.7 cm × 6.7 cm FR4 circuit board

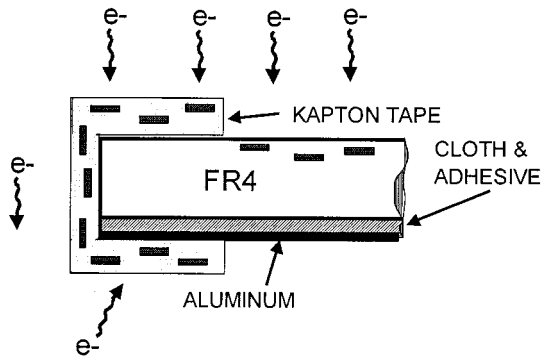

Fig. 10. Cross section view of 0.06-cm FR4 samples with Kapton tape wrap. The tape at the rear of the sample is charged by electrons scattered off the vacuum chamber walls.

under 30 keV electrons, 0.1 nA/cm^2, edges of boards wrapped with Kapton tape.

These samples are not identical to the samples in the first through third geometries thus making direct comparison risky. Besides being a thinner FR4 board, insulating Kapton tape was wrapped around the edges of these samples and over a portion of the electrode on the rear of the sample. The Kapton introduces new discharge characteristics. The surface of the kapton over the sample electrode becomes charged by scattered electrons, and forms an additional charged capacitance of approximately 170 pF. This capacitance adds more charge to the discharge pulses. Fig. 10 describes the effect of the Kapton tape.

Therefore, these samples were also tested under the planar 90% transmission grid just to make proper comparison between conical and planar grids. The results with the 90% transmission plane-parallel grid are provided in Table V.

Comparing pulses in Table V with pulses in Table IV indicates that the conical grid produces significantly larger and more rapid pulses than the planar grid. Fig. 11 indicates a typical pulse under the 60% transmission conical grid (arrangement 4) compared to one under the 90% transmission plane parallel grid (arrangement 1). The hypothesis that divergent fields develop stronger discharges may explain the data. The hypothesis that a more dense grid confines the diffuse gas to generate a stronger discharge conductance may also explain the data. Both effects may be active under the conical grid.

E. Guarding Discharge Current from the Back Electrode

In all of the prior experiments, it is possible that some of the discharge current passed around the edge of the sample to arrive directly on the back electrode. This current flow would produce a *negative* voltage on the 50-Ω scope. It would effectively cancel some of the signal generated by the discharge current that was flowing to the chamber walls. An experiment was designed to determine whether significant current passed directly to the sample electrode.

A sheet of aluminum foil was taped to the edges of the thick FR4 samples, and connected to the walls of the mounting structure. The scheme is described by Fig. 12. By blocking the passage of discharge current to the rear electrode, one would increase the average amplitude of pulses.

TABLE V
PULSES UNDER 90% TRANSMISSION PLANE-PARALLEL GRID, 0.06 cm FR4

Pulse number 11/5/99	Width at half peak (ns)	Peak current 50 ohm (A)	Charge (Coulombs)	Energy in 50 ohms (mJ)
1:36:40	106	13	2.1E-06	0.66
1:37:28	98	12	1.7E-06	0.48
1:38:28	116	8	1.2E-06	0.24
1:44:19	122	12	2.1E-06	0.63
1:46:33	68	11	1.5E-06	0.35
1:47:53	144	6	1.1E-06	0.18
1:51:23	168	10	2.1E-06	0.60
1:56:05	160	6	1.1E-06	0.18
1:57:39	140	12	2.1E-06	0.53
1:59:12	94	14	2.1E-06	0.81
2:03:57	196	9	2.1E-06	0.50
2:06:24	130	9	1.5E-06	0.35
2:06:45	122	10	1.5E-06	0.32
2:09:08	180	9	2.0E-06	0.50
2:13:46	136	8	1.5E-06	0.26
2:14:07	152	11	2.1E-06	0.56
2:14:18	160	6	1.3E-06	0.23
2:20:14	138	12	2.5E-06	0.86
2:22:03	154	6	1.3E-06	0.24
2:24:05	90	16	2.2E-06	0.92
2:26:00	142	12	2.4E-06	0.70
2:29:15	158	6	1.2E-06	0.20
2:30:10	148	7	1.3E-06	0.21
2:31:11	164	11	2.2E-06	0.61
2:36:03	142	7	1.2E-06	0.23
2:36:44	110	15	2.5E-06	0.84
Average	136	10	1.8E-06	0.47

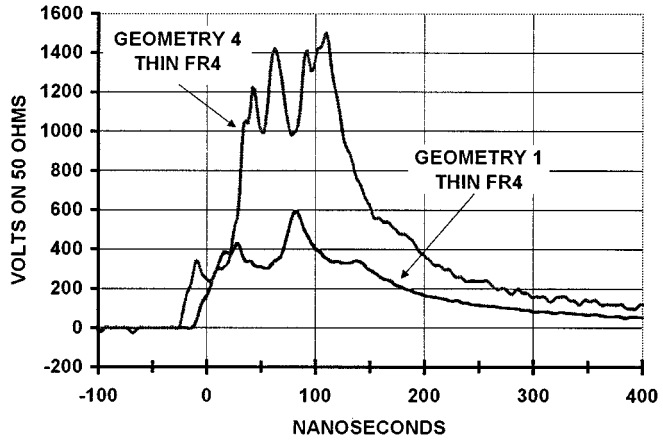

Fig. 11. Comparison of pulse under arrangement 1 (planar open grid) with pulse under arrangement 4 (conical grid) for 0.06 cm FR4.

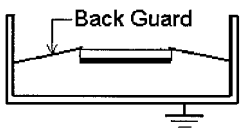

Fig. 12. Aluminum Foil Prevents Discharge Current from Accessing the Electrode.

The results of this test, performed on June 2, 2000, on the same thick FR4 boards is indicated in the last row of Table VI. There were 53 pulses using 30-keV electrons at 0.5 nA/cm^2. It is clear that if charge current did flow directly to the rear electrode, it was small in amplitude. These pulses are not larger than the prior pulses, and in fact were slightly smaller in total charge.

IV. SUMMARY AND DISCUSSION OF RESULTS

The results of these tests are summarized in Table VI. The data for thick samples should not be compared directly to data for thin samples. Thin samples have more capacitance and stored energy for the same surface voltage. For each type of sample one compares the effects of the changes in electrode/chamber arrangement. Fraction of voltage lost cannot be estimated for the thin samples because the initial static voltage on the kapton tape at the rear of the samples was not determined.

The most important parameters for spacecraft design purposes are the peak current and the energy delivered to the (50 Ω) circuit. Peak current changes a factor of four, and energy to the load changes a factor of eight as the chamber electrode arrangement changes. Even more severe changes are discussed below.

It is evident that the pulsed current waveform from spontaneous pulsed discharge of irradiated insulators in vacuum depends upon the interplay between the arrangement of electrodes and (gas?) discharge phenomena. Reference [23] found that every pulse was associated with measurable amounts of gas which created secondary discharges elsewhere in the chamber. Contrary to some reports, our pulses cannot be explained by spontaneous emission of electrons from the surface of the insulator accelerating across the vacuum space. If simple electron emission were the discharge process, one would expect the highest field arrangement (Fig. 3), to produce the fastest and strongest pulses, yet this arrangement produces the weakest pulses. It is difficult to theoretically imagine a cause for sudden emission of electrons at high current density from a planar insulating dielectric.

The discharges occur such that the pulses often do not become well organized. Instead, the discharge process extinguishes prior to fully discharging the surfaces. Consistently after the pulse, samples maintain 3 kV or more as noted by many workers [4]–[8], yet this parameter has never been systematically tabulated in the literature. How the arrangements of electrodes and insulators on actual spacecraft affect the level of threat presented to spacecraft by the discharges is yet to be determined.

Such studies require considerable patience. Time in vacuum is often important for the production of consistent pulsing. Some materials produce no pulses for the first few days of irradiation until conductive ions such as OH out-gas from the sample. Often during the first few days in vacuum the samples produce small pulses amongst the larger pulses. After a few days, the FR4 pulses became very consistent as indicated in the tables. Table V indicates the most pulse variability in this report and has the shortest out-gassing time of three days. Additionally, one should consider the electric field profile developed in the sample by performing studies as in [22]. Some sample geometries and radiation spectra may not develop sufficient electric field inside the insulator to generate pulses. Radiation adds mobile (conducting) radicals in some materials (example PTFE)

TABLE VI
SUMMARY OF AVERAGE PULSE RESULTS

Arrangement And Sample	Peak Current (Amps)	Pulse Width Half Max (ns)	Pulse Energy in 50 Ohms (mJ)	Charge (Coulombs)	Estimated Fraction Surface Volts Lost
Planar Grid 90% Xmsn Thick FR4	5.8	228	0.23	1.33E-06	0.36
Planar Grid 32% Xmsn Thick FR4	20.7	77	1.10	1.85E-06	0.51
Fully Open Center Chmbr Thick FR4	25.0	54	1.20	2.1E-06	0.77
Planar Grid 90% Xmsn Thin FR4	10.0	136	0.47	1.8E-06	?
Conical Grid 60% Xmsn Thin FR4	31	122	3.9	2.9E-06	?
No Grid Back Guard Thick FR4	6.84	123		1.03E-06	

which accumulate to prevent or decrease pulsing after extended exposure [14].

It is possible to extrapolate the findings to predict interesting cases. One can arrange electrodes and use batteries in the several hundred volt range in order to cause the discharge to evolve into hundreds of amperes below a kilovolt, even down to 100 V [23]. The effect described in [23] has serious consequences for power distribution voltage of 100 V or more on spacecraft. Therefore the results presented in this study do not define the extreme situations. This study concerned only the energies associated with the static charge.

One may extrapolate from the results in Tables I–IV to better confine and develop the gas discharge on a spacecraft. Consider a closed, or nearly closed, cavity made of insulator as in Fig. 13. This corresponds to objects such as an integrated circuit package, perhaps the inside of an electronic box, or a covered patch antenna. A discharge inside the cavity confines the gas thereby making larger pulses, and may confine all of the pulse current to flow through sensitive circuits in order to reach ground. In such a case of a patch antenna covered by thermal control blanket, an extremely strong and rapid pulse developed, shown in Fig. 14. This pulse would probably have been much larger if the capacitance of the system had not been so small. Much more study needs to be done in order to tabulate the worst cases for spacecraft applications.

The field of gas discharges is as old as the field of electricity. We have performed this study despite our lack of knowledge of the extensive data about gas discharges. Although we are aware of gas discharge switches, gas lighting, gas voltage regulators, gas rectifiers, and other gas discharge devices, in our study we do not know what gas we have. Nor do we know the density of the gas, nor its initial temperature. From energy constraints not discussed here the ionized fraction of gas initially issued into the vacuum is estimated to be around 1%. One concept for the source of gas is introduced in [16], [22], [23]. That it contains monomers from the polymer insulation is known [20]. Probably those with knowledge of gas discharge physics can improve the analysis of these pulses, but complete understanding hinges on knowing how the gas is generated.

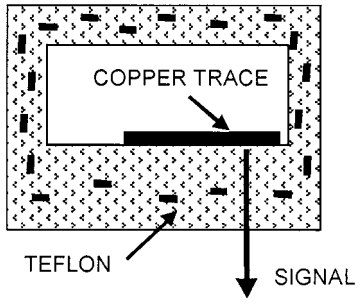

Fig. 13. The arrangement of a circuit inside a charged insulator. A discharge inside the cavity will produce only a negative pulse at the copper trace.

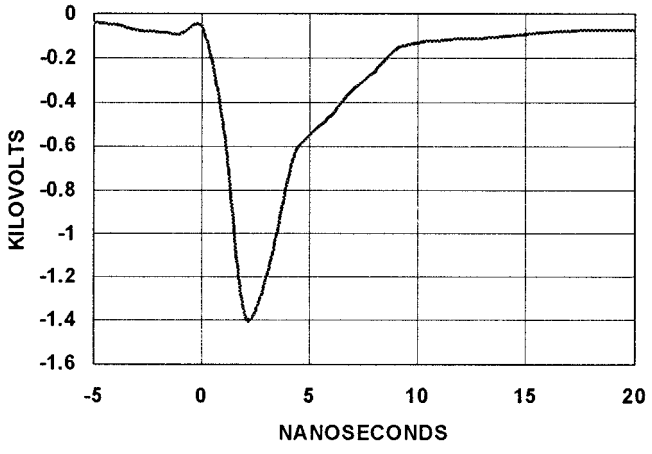

Fig. 14. Pulse generated on 50 Ω when electrode is entirely surrounded by insulator. The capacitance of the system was small but unknown. Note that the pulse was well formed with very high slew rate.

One wishes to provide guidelines for the pulses occurring in spacecraft. Future work is mostly aimed in that direction. At this time it appears that defining the gas discharge as a time dependent resistance is the best one can do. How much current will flow to each specific trace on a circuit board? How much current will flow to a specific node in an integrated package? What is the maximum voltage that will develop on a high-impedance node? Are the gas discharge processes different for other materials in the various geometries? These and other questions require answers.

Note that the voltages driving the discharge are of order 10 kV. The currents are of order 10 A. This means that the resistance of the gas-plasma is of order 1 kΩ. Therefore, the pulse energy delivered to circuits with resistance of order 1 kΩ will increase about a factor of ten over the energy delivered to 50 Ω. The peak voltage on higher impedance circuits above 1 kΩ can rise to order 10 kV. Both of these extremes are serious threats to spacecraft electronics.

For other samples the threat can be crudely estimated. The slew rate is controlled by gas discharge dynamics, and slew rates in Figs. 11 and 13 indicate the range of slew rates to be expected. Discharging surfaces are charged initially to order V = 10 kV, and have a capacitance, C, to the sample electrodes. Typically, CV is discharged by half during a pulse with the current pulse shapes and slew rates chosen from Figs. 11 and 13. The largest pulses come from the samples with largest CV product.

The pulses occurring in these tests are as large as, or worse than, the pulses which occur with people walking on a rug and then discharging to an electronic circuit. But how often they occur on spacecraft we can only estimate [24]. We do know that in the magnetospheres of Earth, Jupiter, and Saturn the high-energy electron fluxes are sufficient to penetrate typical spacecraft surfaces and produce a problem [25]. In deep space and at other planets the environment is less problematic.

APPENDIX
ROUGH ESTIMATES OF GAS EFFECTS

A. Effect of Electric Field Upon Escape of Neutral Molecules

This is an experimental work, and there is no intention to prove or disprove any theory. The discussion is only meant to help the reader hold the experimental results in a conceptual framework. The authors have hypothesized that the electric field in arrangement 3 (Fig. 7), and to a smaller extent in arrangement 4 (Fig. 9), slows or constrains neutral molecules from escaping to the chamber walls thus allowing higher gas density to produce a stronger Townsend discharge. We have not *proved* the hypothesis, but the experimental data does lend support to the hypothesis.

Exact calculations are tedious, but order of magnitude estimates are informative. Assume a small spherical sample of radius r_0 in a large grounded vacuum chamber of radius r_C, and no other electrodes. The electron beam has charged the sample to 20 kV. The electric field inside the sample has initiated a breakdown streamer which begins to emit partially ionized (1% to 10%) gas into the vacuum. The gas expands and cools as it escapes the surface. What work, ΔT, is done by the electric field acting on the neutral molecule as the molecule moves toward the spherical chamber walls?

Let: F_r be the radial force on the neutral gas molecule, p be the dipole moment of the molecule, and E_r be the electric field in vacuum as a function of radial position r. The change in energy, ΔT, of the molecule moving from r_0 to r_C is given by

$$\Delta T = \int_{r_0}^{r_C} F_r \, dr = \int_{r_0}^{r_C} \left(p \frac{d}{dr} E_r \right) \, dr.$$

The electric field is entirely radial

$$E_r = \frac{Q}{(4\pi\varepsilon) r^2}.$$

The sample is charged to V_0 = 20 kV

$$V_0 = \int_{r_0}^{r_C} E_r \, dr.$$

For $r_C \gg r_0$ one obtains

$$\frac{d}{dr} E_r \approx \frac{-2 V_0 r_0}{r^3}.$$

Thus our result is

$$\Delta T \approx \frac{V_0 p}{r_0}.$$

Assume r_0 = 1 cm. For large organic molecules up to 100 Å,

$$p \approx 1 \times 10^{-6} \; electron - cm \text{ so that } \Delta T \approx 0.02 \, \text{eV}.$$

For typical small, 10 Å, organic molecules,

$$p \approx 1 \times 10^{-7} \; electron - cm \text{ so that } \Delta T \approx 0.002 \, \text{eV}.$$

At room temperature the energy in the radial direction, kT/2, is about 0.013 eV.

Therefore, large molecules may be prevented from reaching the chamber walls, and small molecules will be slowed. The real situation is much more complicated. From this limited perspective the hypothesis is reasonable.

B. Transit Time for Electrons and Protons Between Vacuum Chamber Wall and Sample in Center of Chamber

Again, we assume a spherical sample in a spherical chamber. Also assume particles leave the sample or chamber walls with nearly zero kinetic energy, and travel radial to the other body. Using Kepler's Third Law, assuming 20 kV on a 5-cm sample in a 50-cm radius chamber, one finds

$$\text{Proton Transit Time} = 1.7 \text{ ms}$$
$$\text{Electron Transit Time} = 40 \text{ ns}.$$

Because the pulses were roughly 54 ns wide, one immediately realizes that contaminants from the walls of the chamber were not an important source of the pulse current in the third arrangement Fig. 6. There is a small current at long times beyond 2 microseconds in the tail of the pulses that might be due to wall contamination or to remnant gas from the sample, or both.

For the arrangements with grids, there could be some current contributed by desorbed grid contaminants while contam-

inants from the chamber walls would experience no acceleration to the sample. But the data shows that the effect of the grids is to decrease the conductance of the discharge relative to the case without grids. Thus, even though the grids can add conducting particles, the loss of particles through the grids exceeds the gain of grid-contaminant particles. Charged particles passing through the grids have fully registered their current, and therefore were not "lost." But neutrals having escaped through the grids are no longer available to participate in the avalanche. Thus, the experimental results are consistent with the concept of a gas originating at the sample, and producing a gas avalanche extending at least 10 cm from the sample. Grids placed near the sample allow neutrals to escape the discharge that otherwise would participate in the avalanche. Also, conical grids that produce divergent electric field appear to better hold the neutrals within the regions of the sample and gas avalanche than do planar grids.

REFERENCES

[1] H. B. Garrett and C. P. Pike, Eds., *Space Systems and Their Interactions with Earth's Space Environment* New York, 1980, vol. 71, American Institute of Aeronautics and Astronautics Progress in Astronautics and Aeronautics.

[2] E. C. Whipple, "Potentials of surfaces in space," *Rep. Progr. Phys.*, vol. 44, pp. 1197–1250, 1981.

[3] H. B. Garrett, "The charging of spacecraft surfaces," *Rev. Geophys. Space Phys.*, vol. 19, pp. 577–616, Nov. 1981.

[4] E. G. Mullen, M. S. Gussenhoven, D. A. Hardy, T. A. Aggson, B. G. Ledley, and E. C. Whipple, "SCATHA survey of high-level spacecraft charging in sunlight," *J. Geophys. Res.*, vol. 91, pp. 1474–1490, Feb. 1986.

[5] *Proc. Spacecraft Charging Technology Conf.*, C. P. Pike and R. R. Lovell, Eds., Feb. 1977, AFGL-TR-77-0051, NTIS #ADA045459.

[6] *Spacecraft Charging Technology-1978*, AFGL-TR-79-0082, NTIS #ADA084626, 1979.

[7] *Spacecraft Charging Technology-1980*, AFGL-TR-81-0270, NTIS #ADA114426, 1981.

[8] *Spacecraft Environmental Interactions Technology*, AFGL-TR-85-0018, NTIS #N85-22470, 1985.

[9] *Spacecraft Charging Technology Conf., 1989*, PL-TR-93-2027, R. C. Olsen, Ed., 1993.

[10] R. C. Olsen, C. E. McIlwain, and E. C. Whipple, "Observations of differential charging effects on ATS-6," *J. Geophys. Res.*, vol. 86, p. 6809, 1981.

[11] H. C. Koons and D. J. Gorney, "Relationship between electrostatic discharges on spacecraft P78-2 and the electron environment," *J. Spacecraft Rockets*, vol. 28, pp. 683–688, 1991.

[12] M. S. Gussenhoven and E. G. Mullen, "Space radiation effects program, an overview," *IEEE Trans. Nucl. Sci.*, vol. 40, pp. 221–227, 1993.

[13] P. G. Coakley, M. J. Treadaway, and P. A. Robinson, "Low flux laboratory test of the internal discharge monitor (IDM) experiment intended for CRRES," *IEEE Trans. Nucl. Sci.*, vol. 32, pp. 4066–4072, Dec. 1985.

[14] A. R. Frederickson, E. G. Holeman, and E. G. Mullen, "Characteristics of spontaneous electrical discharging of various insulators in space radiations," *IEEE Trans. Nucl. Sci.*, vol. 39, pp. 1773–1782, Dec. 1992.

[15] E. P. Wenaas, M. J. Treadaway, T. M. Flanagan, C. E. Mallon, and R. Denson, "High-energy electron-induced discharges in printed circuit boards," *IEEE Trans. Nucl. Sci.*, vol. 26, pp. 5152–5155, Dec. 1979.

[16] K. G. Balmain and G. R. Dubois, "Surface discharges on Teflon, Mylar, and Kapton," *IEEE Trans. Nucl. Sci.*, vol. 26, pp. 5146–5151, 1979.

[17] T. M. Flanagan, R. Denson, C. E. Mallon, M. J. Treadaway, and E. P. Wenaas, "Effect of laboratory simulation parameters on spacecraft dielectric discharges," *IEEE Trans. Nucl. Sci.*, vol. 26, pp. 5134–5140, Dec. 1979.

[18] B. C. Passenheim, V. A. J. van Lint, J. D. Riddell, and R. Kitterer, "Electrical conductivity and discharge in spacecraft thermal control dielectrics," *IEEE Trans. Nucl. Sci.*, vol. 29, pp. 1594–1600, Dec. 1982.

[19] A. R. Frederickson, "Upsets related to spacecraft charging," *IEEE Trans. Nucl. Sci.*, vol. 43, pp. 426–441, 1996.

[20] R. C. Hazelton, R. J. Churchill, and E. J. Yadlowski, "Measurements of particle emission from discharge sites in teflon irradiated by high energy electron beams," *IEEE Trans. Nucl. Sci.*, vol. 26, pp. 5141–5145, Dec. 1979.

[21] J. P. Marque, "Phenomenology of e-irradiated polymer breakdown," *Vacuum*, vol. 39, pp. 443–452, 1989.

[22] A. R. Frederickson, "Electric discharge pulses in irradiated solid dielectrics in space," *IEEE Trans. Elect. Insul.*, vol. 18, pp. 337–349, June 1983.

[23] A. R. Frederickson, L. Levy, and C. L. Enloe, "Radiation-induced electrical discharges in complex structures," *IEEE Trans. Elect. Insul.*, vol. 27, pp. 1166–1178, Dec. 1992.

[24] A. R. Frederickson, "Method for estimating spontaneous pulse rate for insulators inside spacecraft," *IEEE Trans. Nucl. Sci.*, vol. 43, pp. 2778–2782, 1996.

[25] H. B. Garrett and A. Hoffman, "Comparison of spacecraft charging environments at Earth, Jupiter and Saturn,". in press.

[26] E. W. Gray, "Vacuum surface flashover: A high-pressure phenomenon," *J. Appl. Phys.*, vol. 58, pp. 132–141, July 1985.

Arthur Robb Frederickson (SM'79) received the B.S. degree in physics from the Rensselaer Polytechnic Institute, in 1963, the M.S. degree in physics from the University of Lowell, and the Ph.D. degree in physics from the University of Massachusetts at Lowell.

He is a Principal Engineer at California Institute Technology and Jet Propulsion Laboratory. He was employed for 31 years at three U.S. Air Force Labs, two years at RPI Linear Accelerator.

C. E. Benson, photograph and biography not available at the time of publication.

E. M. Cooke, photograph and biography not available at the time of publication.